Structural Analysis from Powder Diffraction Data
The Rietveld Method

Ecole Thématique : Cristallographie et Neutrons (1997)[1]

JUAN RODRIGUEZ-CARVAJAL
Laboratoire Léon Brillouin (CEA-CNRS), CEA/Saclay
91191 Gif sur Yvette Cedex, France

The Rietveld Method (RM) is being used from 1969, then this year is the 28th anniversary of the famous paper introducing the technique, by H.M. Rietveld, in Journal of Applied Crystallography. During the last 18 years many crystal and magnetic structures have been refined using this method. Neutron powder diffraction (NPD) is the most advantageous technique for using the RM due to the simple peak shape produced by the relatively coarse resolution of neutron diffractometers.
In these notes we give a short review, at an introductory level, of some topics concerning the study of crystal structures by means of neutron powder diffraction. A summary of the relevant scattering formulae used the analysis of powder diffraction data is given. The use of neutron powder diffraction for determining crystal structures of defective materials is illustrated in different cases. Particularly important is the extension of the Rietveld method to investigate the microstructure of solids where the defects cause an anisotropic broadening of the Bragg reflections.

(1) These notes are based on other courses given by the author. In particular some parts of the text have been borrowed from:
"Neutron Powder Diffraction for the Characterization of Structural Defects in Crystalline Solids", by J. Rodríguez-Carvajal, in “Defects and Disorder in Crystalline and Amorphous Solids”, pp 137-156, Nato ASI Series C, Vol 418, Ed. C.R.A. Catlow, Kluwer Academic Publishers.
"Neutron Diffraction from Polycrystalline Materials", by J. Rodríguez-Carvajal, in Lecture Notes of the First Summer School on Neutron Scattering, pp 73-95, August 15-21 1993, Zuoz, Switzerland. Ed. A. Furrer, Paul Scherrer Institut, ISSN 1019-6447.

1. Introduction.

Neutron scattering is a very powerful tool for the study of condensed matter from many points of view. The thermal neutron is a particle that allows the study of both structural and dynamical aspects of matter, due to its unique features: absence of electrical charge, wavelength comparable to that of interatomic distances, energy of the order of of the energy of thermal excitations (phonons and magnons) and magnetic moment.
In these notes the structural aspects of crystalline solids will be stressed. For this reason the dynamical and magnetic aspects of the neutron-matter interaction will not be discussed. The problem to be addressed is that of obtaining quantitative information about the crystal structure and nature and concentration of structural defects in crystalline solids. It is assumed that readers know the elementary theory of diffraction, the reciprocal lattice concept and the fundamentals of crystallography.
X-ray and neutron diffraction techniques provide quantitative statistical information on crystal structures and defects averaged over volumes from about 10^{-3} to a few cm^3, respectively. Electron diffraction and microscopy probe volumes of many orders of magnitude smaller than X-rays or neutrons (10^{-19}- 10^{-17} cm^3). This fact is important in correctly interpreting the nature of the information provided by the different diffraction techniques.

The notes are organized as follows: in the first part, the theoretical background of diffraction by crystalline solids, eventually with structural defects of different types, will be summarized. In the second part the intensity formulae for the powder method are emphasized with the discussion of the fundamentals of the Rietveld Method (RM). In the third part we give a short presentation of the resolution requirements of a two-axis neutron diffractometer to be useful for crystal structure refinements and for the so called *ab initio* structure determination. In the third part, different types of approximation used in studying real materials by means of Neutron Powder Diffraction (NPD) are described. In particular the cases where the shape of Bragg reflections contains useful information because it is strongly affected by the interaction between defects. For instance, isotropic and anisotropic broadening due to small coherence length of domains and strains produced by defects. The extended Rietveld method is the most powerful tool for refining simultaneously a structural and a microstructural model. The structural model is given by the standard crystallographic parameters and the microstructural model is characterized by a shape and width of reflections depending on *hkl* indices through size and strain parameters. Several examples will be presented and discussed in some detail for oxides of the family $Ln_{2-x}Sr_xNiO_{4\pm\delta}$.

1. Theoretical Background of Scattering from Polycrystalline Materials.

In scattering experiments, the incident particle (neutron, electron, photon...) experiences a change in its momentum and energy. In neutron scattering the quantities:

$$(h/2\pi)\mathbf{Q} = (h/2\pi)(\mathbf{k}_F - \mathbf{k}_I) = h\,\mathbf{s} \qquad h\nu = E_F - E_I$$

represent the momentum and energy change experienced by the particle in the interaction with the target. F and I subscripts stand for final and initial state of the particle, respectively. The wave vector of the particle is the conventional definition, ($k=2\pi/\lambda$) and the energy is the classical kinetic energy ($E= ½ m v^2$). In the following we shall be concerned with elastic scattering ($h\nu==0$) for which $|\mathbf{k}_F|=|\mathbf{k}_I|= 2\pi/\lambda$ and $|\mathbf{Q}|= Q = (4\pi/\lambda) \sin\theta$, θ being half the scattering angle. In these notes we shall use, either the scattering vector used by neutronists, **Q**, or the conventional "crystallographic scattering vector" $\mathbf{s} = \mathbf{Q}/2\pi$.

In this section we shall give a short review of the scattering formulae to be applied in the study of crystal structures by diffraction methods. The reader interested in a deep understanding of the scattering by crystalline matter with defects must consult the literature and particularly the three books of Guinier, Warren and Cowley[1] respectively, on which most of the following theoretical discussion is based. For a theoretical treatment of all aspects of neutron scattering see the books from Lovesey[1].

In the kinematic theory (first Born approximation), the amplitude of the wave scattered by an object is the Fourier transform (FT) of its scattering density (SD) $\rho(\mathbf{r})$ measured in cm^{-2}. The SD means different things for each kind of scattered radiation (X-rays, neutrons and electrons). Any object can be considered as constituted by atoms of SD $\rho_{aj}(\mathbf{r})$ centered at positions $\mathbf{R}_j$; the SD and the corresponding scattered amplitude and intensity can be written as:

$$\rho(\mathbf{r}) = \sum_j \rho_{aj}(\mathbf{r}-\mathbf{R}_j) \qquad [1]$$

$$A(\mathbf{s})= \int \sum_j \rho_{aj}(\mathbf{r}-\mathbf{R}_j) \exp\{2\pi i \mathbf{s}\mathbf{r}\} d^3\mathbf{r} = \sum_j \exp\{2\pi i \mathbf{s}\mathbf{R}_j\} \int \rho_{aj}(\mathbf{u}) \exp\{2\pi i \mathbf{s}\mathbf{u}\} d^3\mathbf{u} \qquad [2]$$

$$A(\mathbf{s}) = \sum_j f_j(\mathbf{s}) \exp\{2\pi i\, \mathbf{s}\, \mathbf{R}_j\} \qquad [3]$$

$$I(\mathbf{s}) = A(\mathbf{s})A(\mathbf{s})^* = \sum_i \sum_j f_i(\mathbf{s})\, f_j(\mathbf{s})^* \exp\{2\pi i\, \mathbf{s}\, (\mathbf{R}_i-\mathbf{R}_j)\} \qquad [4]$$

The last two formulae are the basis for the structural study of any kind of material by elastic scattering. The scattering factor of the atoms $f_j(\mathbf{s}) = FT[\rho_{aj}(\mathbf{r})]$, given in units of length, is the link between the fundamental interaction of each particular radiation with matter. The different ways of writing the equation [4] provide specific and simplified formulae for each kind of idealized or defective structure and for different experimental conditions.

For powders, we have to average the intensity for all possible orientations of an object with respect to the incident beam. The intensity depends on the length, s, of **s** and the whole set of interatomic distances $R_{ij}=|\mathbf{R}_i-\mathbf{R}_j|$; and is given by the Debye formula in terms of $Q=2\pi s$:

$$I(Q) = \sum_i \sum_j f_i f_j \sin\{QR_{ij}\}/(QR_{ij}) \qquad [5]$$

If we consider the thermal motion of the atoms it is easy to show that the equations [3] and [4] hold by substituting the scattering factors by $f_i(\mathbf{s})\exp[-W_i(\mathbf{s})]$. Here the exponential function is called the temperature or Debye-Waller factor. In the harmonic approximation $W_i(\mathbf{s})$ can be written in matrix form as[2]: $W_i(\mathbf{s}) = 2\pi^2\mathbf{s}^T\langle\mathbf{u}_i\mathbf{u}^T{}_i\rangle\mathbf{s}$, where **u** is the column vector of atomic displacements and the superscript ^{T} denotes transpose. For simplicity, if not given explicitly, the temperature factors are considered to be included in the scattering factor. Other kinds of scattering due to thermal motion, e.g. thermal diffuse scattering (TDS), have to be added to equations [4-5] but will not be considered here.

A particularly useful language to describe the diffraction phenomena is that of convolutions and distributions. This is illustrated in the following paragraph.

If crystalline matter is considered as an infinite assembly of unit cells with scattering density $\rho_c(\mathbf{r})$ (=0, for **r** outside the unit cell), the total scattering density of the infinite object can be decomposed in the following way:

$$\rho_\infty(\mathbf{r}) = \sum_n \rho_c(\mathbf{r}-\mathbf{R}_n) = \rho_c(\mathbf{r}) * \sum_n \delta(\mathbf{r}-\mathbf{R}_n) = \rho_c(\mathbf{r}) * z(\mathbf{r})$$

where, $*$ denotes convolution product, $\delta(\mathbf{r})$ is the Dirac function, $\mathbf{R}_n$ is the vector position of the n-th unit cell (direct lattice vector) and $z(\mathbf{r}) = \sum_n \delta(\mathbf{r}-\mathbf{R}_n)$ is the distribution function of an infinite lattice. For a finite crystal $z(\mathbf{r})$ must be replaced by $z(\mathbf{r})g(\mathbf{r})$, where $g(\mathbf{r})$ is the shape factor of the crystal defined as $g(\mathbf{r})=1$ for **r** inside the crystal, and $g(\mathbf{r})=0$ for **r** outside. The scattered amplitude for a finite crystal is:

$$A(\mathbf{s})=FT\{\rho_f(\mathbf{r})\}=FT\{\rho_c(\mathbf{r})*z(\mathbf{r})g(\mathbf{r})\}= F(\mathbf{s})\, Z(\mathbf{s})*G(\mathbf{s})=F(\mathbf{s})/V_c \sum_{\mathbf{H}} G(\mathbf{s}-\mathbf{H}) \quad [6]$$

where $F(\mathbf{s})$ is the structure factor of the unit cell, which can be formally written as equation [3] but with the sum extended to the atoms of a single unit cell. Z denotes the FT of z, and G the FT of g. It can be demonstrated that $Z(\mathbf{s}) = 1/V_c \sum_{\mathbf{H}} \delta(\mathbf{s}-\mathbf{H})$, where V_c is the volume of the unit cell and **H** is a

reciprocal lattice vector. That is the justification of the last equality in [6]. $G(\mathbf{s})$ is a delta function for an infinite crystal, in that case the equation [6] expresses the fact that scattering exists only in the direction $\mathbf{k}_F=\mathbf{k}_I+2\pi\mathbf{s}$, for orientations of the crystal with respect to the incoming beam satisfying the Laue condition $\mathbf{s}=\mathbf{H}$. This can be geometrically illustrated by the well known Ewald construction: a diffracted beam exists only if there is a

node of the reciprocal lattice in contact with the Ewald sphere. The Bragg law is a consequence because $s=|\mathbf{s}|=2\sin\theta/\lambda$, and $|\mathbf{H}|=1/d_{hkl}$. If the sample is present as a crystalline powder, all the orientations are available and the reciprocal lattice can be represented by a set of concentric spheres intersecting the Ewald sphere; and giving rise to diffracted beams in cones .

For a finite crystal, of volume V, constituted by a sufficient number, N, of unit cells, $G(\mathbf{s})$ is different from zero only in the vicinity of the origin. The intensity is given by:

$$I(\mathbf{s})=F^2(\mathbf{s})/V^2_c \sum_{\mathbf{H}}G(\mathbf{s}-\mathbf{H}) \sum_{\mathbf{H}'}G^*(\mathbf{s}-\mathbf{H}')\approx NF^2(\mathbf{s})/(VV_c)\sum_{\mathbf{H}}G^2(\mathbf{s}-\mathbf{H}) \qquad [7]$$

For finite crystals the intensity distribution in reciprocal space is determined by the square of the FT of the shape factor $G^2(\mathbf{s}-\mathbf{H})$. The region around each reciprocal lattice point, where $G^2(\mathbf{s}-\mathbf{H})$ is significantly different from zero, is called a "reflection domain". If the crystal has a plate-like shape the reflection domain is a sort of "cigar" perpendicular to the basal planes. The smaller the thickness of the platelet, the longer is the cigar. For a two dimensional crystal the diffraction domains are infinite rods.

The finite size of a crystal is an unavoidable defect. If the crystals of a powder are very small the diffraction pattern shows broadened peaks.

It can be demonstrated that the function $G^2(\mathbf{s})$ is the FT of the autocorrelation of the shape factor defined as:

$$V\cdot\eta(\mathbf{r})=\int g(\mathbf{u})g(\mathbf{r}+\mathbf{u})d^3\mathbf{u} \qquad [8]$$

The interpretation of $\eta(\mathbf{r})$ is straightforward: it represents the fraction of the total volume shared in common between the object and its "ghost" displaced by the vector $\mathbf{r}$. Obviously, $\eta(0)=1$ and decreases as $\mathbf{r}$ increases (see figure 1).

Crystalline defects can be of many different types: point defects such as vacancies and interstitials, clusters of point defects, displacement and substitutional disorder, microdomains, twinning, microtwinning, intergrowth, stacking faults, antiphase domains, and strain fields due to all kinds of imperfections. However, in many defective crystals it is always possible to define an average lattice.

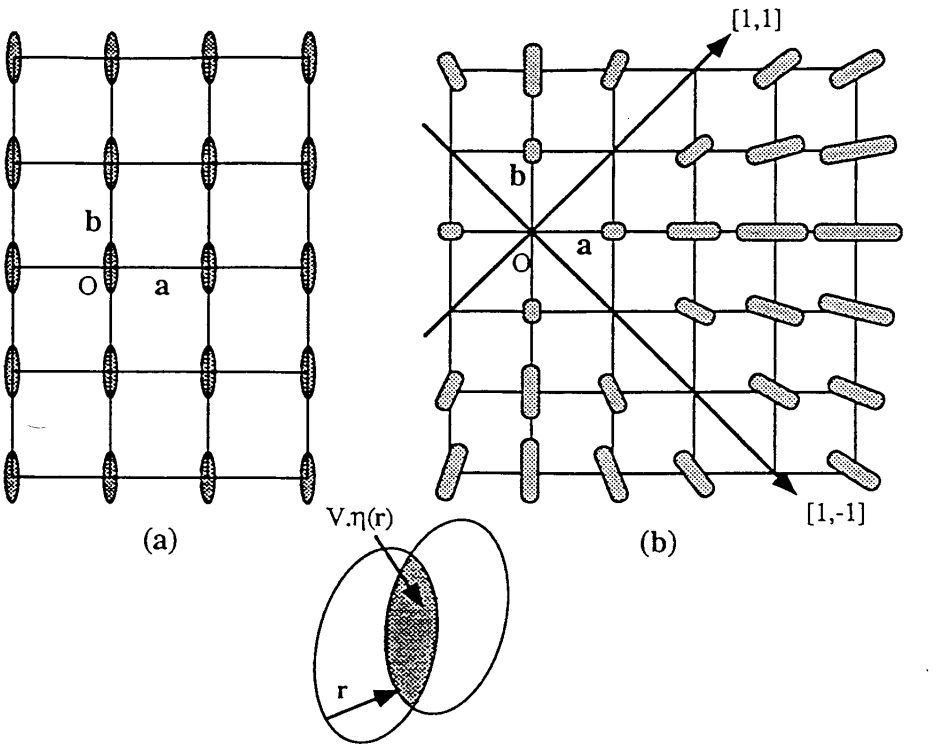

*Figure 1: Two dimensional representation of the intensity distribution in reciprocal space for the case of (a) small crystallites without defects and (b) a defective material in which the strong correlation between defects produces an anisotropic broadening of Bragg reflections. A scheme for the interpretation of the V.h(**r**) function is also shown.*

In such cases, the structure factor of each unit cell can be different and the equation [4] holds by substituting the structure factor of each cell for the scattering factors of the atoms. The position vectors become vectors of the average lattice. Furthermore, the intensity formula can be rewritten as:

$$I(\mathbf{s}) = \sum_n (\sum_m F_m F^*_{m+n}) \exp\{2\pi i\, \mathbf{s}\, \mathbf{R}_n\} \qquad [9]$$

Taking into account the long range homogeneity of the object, the average value $p_n=\langle F_m F^*_{m+n}\rangle$ is independent of m. The number of terms in the inner sum of [9] is given by $V\eta(\mathbf{R}_n)/V_c$ and the equation [9] can be transformed to:

$$I(\mathbf{s}) = V/V_c \sum_n \eta(\mathbf{R}_n)\langle F_m F^*_{m+n}\rangle \exp\{2\pi i\, \mathbf{s}\, \mathbf{R}_n\} = N \sum_n \eta(\mathbf{R}_n)\, p_n \exp\{2\pi i\, \mathbf{s}\, \mathbf{R}_n\}$$

If we define the average structure factor as $F=\langle F\rangle = 1/N \sum_m F_m$, and write $\phi_n=F-F_n$, it is easy to see that $p_n=F^2+\langle \phi_m \phi^*_{m+n}\rangle = F^2+\Phi_n$, and the intensity formula [10] can be further decomposed in two terms:

$$I(\mathbf{s}) = I_{Bragg}+I_{Diffuse} = N F^2 \sum_n \eta(\mathbf{R}_n) \exp 2\{\pi i\, \mathbf{s}\, \mathbf{R}_n\} + N \sum_n \eta(\mathbf{R}_n)\, \Phi_n \exp\{2\pi i\, \mathbf{s}\, \mathbf{R}_n\}$$

$$= \quad N F^2/(VV_c) \sum_{\mathbf{H}} G^2(\mathbf{s}-\mathbf{H}) \quad + \quad N \sum_n \Phi_n \exp\{2\pi i\, \mathbf{s}\, \mathbf{R}_n\}$$

In the last expression, we have made the approximation $\eta(\mathbf{R}_n)=1$ because Φ_n decreases with n faster than $\eta(\mathbf{R}_n)$. If the correlations between different unit cells are weak, the main term contributing to the "diffuse scattering" is n=0. In that case we have $I_{Diffuse}=N\{\langle F^2\rangle-\langle F\rangle^2\}$. When correlations between fluctuations are strong up to a sufficient number of unit cells, Φ_n decreases slowly with n, and the intensity is concentrated around the nodes of the average reciprocal lattice. The result is a broadening of the Bragg reflections and the separation between diffuse and sharp scattering is not so clear-cut. In general the function $\Phi_n=\Phi(\mathbf{R}_n)$ depends also on the scattering vector **s** and can even be a periodic function giving rise to the appearance of satellite peaks characteristic of modulated structures.

The formulae given above are very general and there are many particular cases in the literature where the expressions can be further developed making explicit the physical magnitudes of interest.

An important situation occurs where the structure factor for the cell m can be written as the average structure factor multiplied by a phase factor of the type $\exp\{2\pi i \mathbf{s}\mathbf{u}_m\}$. That means the effect of the structural defects is manifested mainly as a "strain" on the average lattice. We have: $F_m=F \exp\{2\pi i\, \mathbf{s}\, \mathbf{u}_m\}$, with the constraint: $\sum_m \exp\{2\pi i\, \mathbf{s}\, \mathbf{u}_n\}=0$. Equation [10] can be written as:

$$I(\mathbf{s}) = N F^2 \sum_n \eta(\mathbf{R}_n)\, \zeta(\mathbf{R}_n, \mathbf{s}) \exp\{2\pi i\, \mathbf{s}\, \mathbf{R}_n\} \qquad [12]$$

where $\zeta(\mathbf{R}_n, \mathbf{s})= \langle \exp\{2\pi i \mathbf{s}(\mathbf{u}_m-\mathbf{u}_{m+n})\}\rangle$. The expression [12] is a quasi-Fourier series. The dependence on **s** of the strain coefficients destroys the similarity. However, if we consider the

scattering in the first Brillouin zone around a Bragg reflection and a smooth variation of ζ with **s**, we can write for $\mathbf{s}=\mathbf{H}+\Delta\mathbf{s}$:

$$I_{\mathbf{H}}(\Delta\mathbf{s}) = N F^2_{\mathbf{H}} \sum_n \eta(\mathbf{R}_n)\, \zeta_{\mathbf{H}}(\mathbf{R}_n) \exp\{2\pi i\, \Delta\mathbf{s}\, \mathbf{R}_n\} \approx F^2_{\mathbf{H}}\, \Omega_X(\Delta\mathbf{s})$$

where $\Omega_X(\Delta\mathbf{s})$ is the "single crystal" intrinsic profile of the Bragg reflection, which is expressed as a Fourier series of coefficients given by a product of size, $\eta(\mathbf{R}_n)$, and strain, $\zeta_{\mathbf{H}}(\mathbf{R}_n)$, coefficients. In order to separate the two effects it is necessary to measure different orders of a reflection, i.e. **H**, 2**H**, 3**H**... A new averaging step is necessary to arrive at the powder expression which is similar to [12] (see, for instance, the book of Warren in reference 1). In theory, the size coefficients for a particular (*hkl*) reflection can provide, through a second derivative, the diameter distribution over the sample, perpendicular to the (*hkl*) planes (see reference 1). A similar case holds for the strain coefficients. In practice, the intrinsic profile is convoluted with the instrumental one, and it is in general very difficult to obtain the Fourier coefficients with sufficient accuracy due to peak overlap. For crystals of low symmetry it is impossible and approximations have to be made.

2. Fundamentals of the Rietveld Method

Equation [11] when developed for a powder with well resolved Bragg reflections, can be written as follows:

$$y_i = \sum_{\mathbf{H}} I_{\mathbf{H}}\, \Omega(T_i - T_{\mathbf{H}}) + D_i + B_i \qquad [14]$$

where y_i is the number of counts, the subscript "i" represents a discrete observation at the scattering variable T_i. Here we adopt the variable T to describe either, the scattering angle 2θ, the time of flight *t* (TOF, if a neutron pulsed source is used) or the scattering vector modulus Q or s. **H** corresponds to Bragg peaks contributing to the channel "i". $I_{\mathbf{H}}$ is the integrated intensity of the reflection **H**, $\Omega(T_i - T_{\mathbf{H}})$ is the value of the normalized profile function of the Bragg reflection at the position T_i due to the reflection **H** at the position $T_{\mathbf{H}}$. D_i, is the diffuse scattering due to defects. Finally, B_i is the background coming from other sources (TDS, incoherent scattering, inelastic, sample environment, etc.).

The diffuse term D contains a spherical average of the second term of equation [11]. A detailed analytical expression for the general case is not very useful, but an approximation consisting in a Debye-like expression holds:

$$D_i = D(Q_i) = \sum_j \alpha_j \sin\{QR_j\}/(QR_j) \qquad [15]$$

The number of terms to be considered in the sum, and the interpretation of the coefficients α_j and distances r_j, depend on the particular defect model. To obtain the maximum information from the powder diffraction data experimentally, absolute values (corrected for inelasticity and sample environment) of the intensities have to be collected in order to be able to separate the different contributions to the intrinsic background. Only under these conditions can the diffuse scattering term be handled quantitatively. Some examples of the use of this term can be found in reference 3.

The information about the average crystal structure is contained in $I_{\mathbf{H}}(\sim F^2)$ and $T_{\mathbf{H}}$ (through the cell parameters). The size and shape of the reflection domains as well as the strains produced by the defects contribute to the profile function $\Omega(T)$.

In modern treatments of powder diffraction patterns the Rietveld method[4] (RM) is commonly used. In the classical RM, the weighted sum of squared difference between y_{iobs} and y_{ical} [14] is minimized. If the set of model parameters is $\boldsymbol{ß} = (ß_1, ß_2, \ldots ß_P)$, the Rietveld method tries to optimize the chi-square function:

$$\chi^2_p = \sum_i w_i \{y_{iobs} - y_{ical}(\boldsymbol{ß})\}^2 \qquad [16]$$

where w_i is the inverse of the variance associated to the observation "i" ($\sigma^2(y_{iobs})$).

The functions I, Ω, D and B, are calculated on the basis of a particular structural model and some empirical functions depending on a number of adjustable parameters.

The integrated intensity for a Bragg reflection is given by:

$$I_{\mathbf{H}} = \{j\ L\ A\ O\ E\ F^2\}_{\mathbf{H}} \qquad [17]$$

where j is the multiplicity, $L=1/(2\sin^2\theta\cos\theta)$ is the Lorentz factor for constant wavelength neutrons, in the case of TOF we have $L=d^4\sin\theta$, A is the absorption correction, O is a function to correct, if needed, for preferred orientation, E is the primary extinction correction and F is the structure factor of the average unit cell. For a review of the RM the reader is referred to the reviews summarized under reference 5.

In the last few years, the RM has been used for the study of crystalline materials with defects, usually handling only the average structure. This can be done in cases where the interaction of the defects does not have a big effect on the shape of Bragg reflections: the profile function and the half-width parameters are not very different from the instrumental ones. The structural parameters are contained in the expression of the structure factor of the unit cell:

$$F(\mathbf{H})=\sum_{r=1,m} n_r\, b_r \sum_{s=1,p} \exp(-\mathbf{H}_s^T\, [\beta]_r\, \mathbf{H}_s) \exp\{2\pi i\, (\mathbf{H}_s^T\, \mathbf{r}_r + \mathbf{H}^T\, \mathbf{t}_s)\} \qquad [18]$$

where the first summation runs over the number m of atoms in the asymmetric unit, p being the number of symmetry equivalent positions, and n_r is the occupation factor of atom r (for a fully occupied site n is the multiplicity of the site divided by p). $\mathbf{H}_s$ is defined as: $\mathbf{H}_s^T = \mathbf{H}^T\, [R]_s$, where $[R]_s$ is the (3x3) matrix representing the rotational part of the symmetry operator s, $\mathbf{t}_s$ is the corresponding translational part. The symmetric (3x3) matrix $[\beta]_r$ represents the anisotropic thermal parameters of atom r; it is related to the displacement matrix by: $[\beta]_r = 2\pi^2 \langle \mathbf{u}_r \mathbf{u}^T{}_r \rangle$, with displacement vectors in fractions of the unit cell parameters.
It is worth mentioning that for defective materials, the occupation factors and the displacement parameters are of major importance. In practice, $[\beta]_r$ contains, not only the thermal vibration of atoms, but also all other static displacements from the ideal positions due to local strains or disorder. The two components, static and dynamic, of $[\beta]_r$ can be distinguished by making the appropriate temperature dependent diffraction experiment. In cases where the scattering density is smeared out due to non-well-localized atoms (for instance, ionic conductors) one can use higher order expansions (as in anharmonic probability density functions)[6] to describe the situation.

The procedure used in practice to minimize the expression [16] is iterative as the problem to be solved is non linear. If the counting statistics follows a Poisson distribution and the count rate is sufficiently high to approach a gaussian, then $\sigma^2_i = y_{iobs}$. The minimum condition of χ^2_p with respect to the parameters **ß** implies that the gradient $\partial\chi^2_p/\partial$**ß** should be zero. A Taylor expansion of y_{ical}(**ß**) around an initial set of parameters $\mathbf{ß_o}$ allows the application of an iterative process. The shifts to be applied to the parameters at each cycle for improving χ^2_p are obtained by solving a linear system of equations (normal equations): A δ**ß** = **b**, where the symmetric matrix A, of dimension P x P, and the vector **b** have as components:

$$A_{kl} = \sum_i w_i\, (\partial y_{ical}\, (\mathbf{ß_o})/\partial ß_k)\, (\partial y_{ical}\, (\mathbf{ß_o})/\partial ß_l) \qquad [19]$$

$$b_k = \sum_i w_i\, \{y_{iobs} - y_{ical}(\mathbf{ß_o})\}(\partial y_{ical}\, (\mathbf{ß_o})/\partial ß_k) \qquad [20]$$

The normal equations of the non linear least square procedure take the form:

$$\sum_l A_{kl}\, \delta ß_l = b_k \qquad [21]$$

the shifts of the parameters obtained by solving [21] are added to the starting parameters giving rise to a new set, $\mathbf{ß_n} = \mathbf{ß_o} + \delta\mathbf{ß}$, wich are closer to the optimum set $\mathbf{ß_m}$. The new parameters are considered as the starting ones in the next cycle and the process is repeated until a convergence criterium is satisfied. The standard deviations of the ajusted parameters are calculated by the expression:

$$\sigma^2(ß_i) = (A^{-1})_{ii}\, \chi^2_v \qquad [22]$$

where $\chi^2_v = \chi^2_p /(N-P)$ is the reduced chi-square.

3.Requirements of powder diffractometers for crystal structure refinement.

We shall be concerned only with high resolution powder diffraction, then the "banana"-type position sensitive detectors which are extremely useful in magnetism and kinetics studies will not be discussed here. In these notes, instrumental aspects of NPD are not treated in detail; the reader is referred to the works of Hewat and David *et al.*[7] for constant wavelength and time of flight diffractometers respectively.

High resolution powder diffractometers, conceived for crystal structure refinements in constant wavelength environment, use Ge-monochromators in order to get the highest intensity at high take-off angle and eliminate $\lambda/2$ contamination. The high take-off angle is needed for matching the best resolution with the highest reflection overlap, which occurs at an angle higher than $2\theta=100°$ (see reference 10).

Using the well known Caglioti's relations one can calculate an approximate resolution function of the two axis diffractometer (Fig. 2). The full width at half maximum (Fwhm) of Bragg reflections varies with the scattering angle, 2θ, following the expression:

$$FWHM(2\theta) = (U\tan^2\theta + V\tan\theta + W)^{1/2} \qquad [23]$$

where the parameters U,V and W can be written in terms of the angular divergence of the incoming neutrons to the monochromator, α_1, the angular aperture of a monochromator-to-sample collimator, α_2, the collimation between sample and detector, α_3, the take-off angle of the monochromator, $2\theta_m$, and its mosaicity, β. The Caglioti-Paoletti-Ricci equations for the parameters U, V and W are:

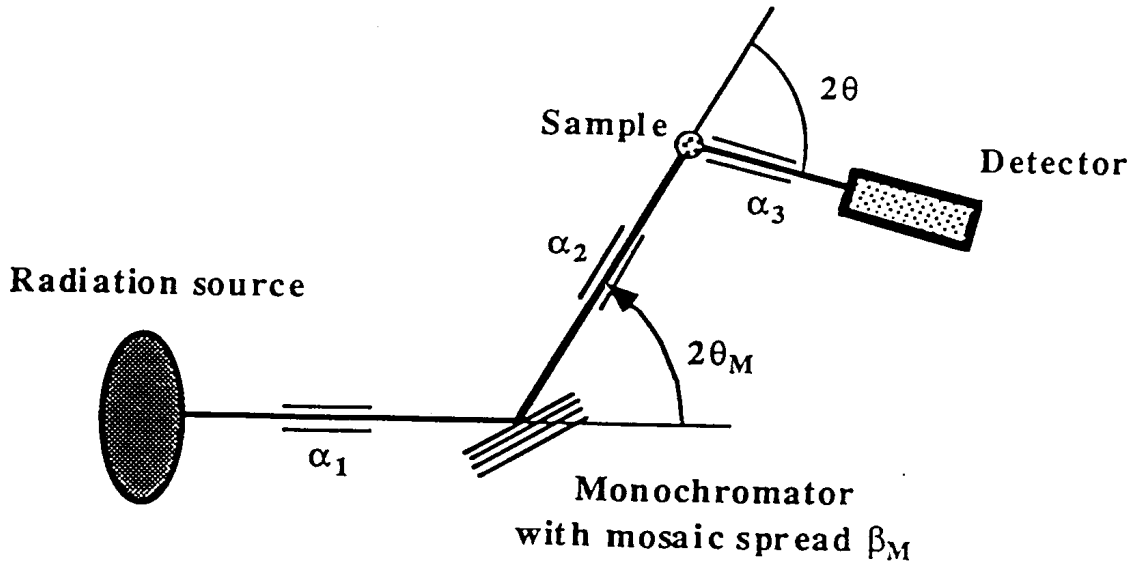

Fig. 2 - Powder diffraction geometry (Caglioti et al.)

$$U = 4(\alpha_1^2\alpha_2^2 + \alpha_1^2\beta^2 + \alpha_2^2\beta^2)/[\tan^2\theta_m\,(\alpha_1^2 + \alpha_2^2 + 4\beta^2)]$$
$$V = -4\,\alpha_2^2\,(\alpha_1^2 + 2\,\beta^2)/[\tan\theta_m\,(\alpha_1^2 + \alpha_2^2 + 4\beta^2)] \qquad [24]$$
$$W = [\alpha_1^2\alpha_2^2 + \alpha_1^2\alpha_3^2 + \alpha_2^2\alpha_3^2 + 4\beta^2(\alpha_2^2+\alpha_3^2)]/(\alpha_1^2 + \alpha_2^2 + 4\beta^2)$$

the minimum of the resolution curve [19] occurs at:

$$\tan\theta = -V/2U = \alpha_2^2\,(\alpha_1^2 + 2\,\beta^2)\tan\theta_m/2(\alpha_1^2\alpha_2^2 + \alpha_1^2\beta^2 + \alpha_2^2\beta^2) \approx \tan\theta_m \qquad [25]$$

the last approximation holds only if $\alpha_1 << \beta,\ \alpha_2$. As discussed in reference 10, the best resolution conditions can be obtained with $\alpha_2 = 2\beta > \alpha_1 \approx \alpha_3$.
For instance, in the case of D1A, at LLB, we have the parameters, $2\theta_m = 131.4$, $\beta \approx 20'$ and $\alpha_3 \approx 10'$. The effective collimation, α_1, can be calculated from the characteristics of the guide (natural Ni) and is given by the expression: α_1(in minutes of arc) = 12' λ (in Å).

What is important to discuss the performance of a powder diffractometer, for structure determination and refinement, is the comparison between the resolution curve and the average separation between adjacent Bragg reflections. In comparing different instruments with different wavelengths the resolution curves must be represented in reciprocal space. As is usual in neutron

scattering literature we shall use the scattering vector modulus $Q=4\pi\sin\theta/\lambda$ as the natural "distance to the origin" in reciprocal space.

We shall establish simple criteria for determining the capability of a powder diffractometer, characterized by its resolution function, in providing good data for structure determination and refinement. In principle the complexity of a crystal structure can be considered as something proportional to the number of free parameters to be refined. The number of free parameters of a crystal structure is a quantity verifying the relation:

$$N_f \approx n\, V_o / j\, V_a \qquad [26]$$

where n is the number of parameters for a single atom (=3 if only atomic positions are considered), V_o is the volume of the *primitive* cell, V_a is the average volume per atom which is always greater than 10 Å^3, j is the multiplicity of the Laue class, i.e. j =2, 4, 8, 12, 16, 24 and 48 for triclinic, monoclinic, orthorhombic, trigonal, tetragonal, hexagonal and cubic systems, respectively. In a diffraction experiment one has to get a number of independent observations (integrated intensities) greater than N_f. Let us call "r" the ratio between the number of reflections required to succeed in the refinement, N_r, and the number of free parameters. Thus we can write the relation:

$$N_r = r\, N_f \qquad [27]$$

The value of "r" is, of course, not determined. However one can safely take a value of r=10, even if much smaller ratios can be satisfactory. From a conservative view one takes the equal sign in the relation [26]. These considerations determine a minimum value of the reciprocal distance, Q_{min}, that a high-resolution powder diffractometer has to reach in order to properly handle the refinement of the crystal structure. The number of independent reflections inside a reciprocal sphere of radius Q verifies the following relation:

$$N(Q) \approx Q^3\, V_o / (\, 6\pi^2\, j) \qquad [28]$$

The sign < comes from the fact that the multiplicity of reflections in the "surface" of the hkl-asymmetric domain (hk0, for instance) is lower than the general multiplicity j. Taking also the equal sign of [28] and putting $N(Q_{min})=N_r$, one obtains:

$$Q_{min} = (6\pi^2\, n\, r / V_a\,)^{1/3} \approx (6\pi^2\, n)^{1/3} \approx (24\pi^2)^{1/3} \approx 6.19\ \text{Å}^{-1} \qquad [29]$$

where the approximations correspond to the values r=10, V_a= 10 Å^3 and, finally, n=4. The quoted value is, perhaps, a little bit high (r could be reduced to 5, Q_{min}=4.91Å^{-1}) and correspond, indeed, to the highest value reachable with the actual configuration of D1A.

Relation [29] puts a limit to the capability of a powder diffractometer for the refinement of a crystal structure. Diffractometer not reaching Q_{min} are not useful for general structure refinements, only simple particular cases can be treated.

The above considerations do not take into account the finite resolution of the diffractometer (in fact the peaks have been considered as Dirac functions). Besides a Q-range given by $(0,Q_{min})$, the reflections should be "well measured". The resolution function of the diffractometer must be capable of separating adjacent reflections in order to get the major fraction of the full set of independent reflections in the available Q-range.

As can be deduced from the expression of Q, the resolution in reciprocal space can be calculated from the angular units (in radians) multiplying the relation [23] by $2\pi\ \cos\theta/\lambda$ and using Q as independent variable instead of 2θ. Let us call D_Q the full width at half maximum expressed in $Å^{-1}$.

Differenciating the equation [28] one can obtain the density of reflections per $Å^{-1}$:

$$dN(Q) = Q^2 V_o/ (2\pi^2 j)\, dQ = \rho(Q)\, dQ = dQ/\Delta(Q) \qquad [30]$$

$$dN(2\theta) = (16\pi V_o / j \lambda^3) \sin^2\theta \cos\theta\, d(2\theta) \qquad [30']$$

the differencial dN(Q) represents the number of reflections within a spherical layer of mean radius Q and thickness dQ. The reciprocal of the density, $\rho(Q)$, is the average separation between reflections, $\Delta(Q)$, along Q. The equation [30'] is given to show that the density of Bragg peaks, in angular units, is proportional to the reciprocal of the Lorentz factor for powders. Thus, the reader can verify that the maximum peak-overlap occurs at $2\theta \approx 109.5$ Coming back to the reciprocal space, we have to establish a criterium for considering that the reflections are "well separated" in the whole Q-range. We can formulate the prescription as follows, the reflections can be discriminated if the following relation holds:

$$\Delta(Q) = 2\pi^2 j / (Q^2 V_o) \approx p\, D_Q \qquad [31]$$

where p is a factor lower than unity. For instance, one can consider that two reflections can be well measured if their positions are separated more than one half their Fwhm, i.e. p=0.5. If we represent in the same graphics the values $\Delta(Q)/p$, for different (j,V_o), and D_Q, is very easy to see what structures can be straightforwardly refined: those keeping $\Delta(Q)/p$ above D_Q in the full Q-range. The above values chosen for the "criteria" parameters: r=10 and p=0.5, are very conservative and lower values imply that more complex structures can be refined. In practice, each particular case should be analysed with care.

As an application of the criteria discussed in the previous paragraph, we have represented in Fig. 3 the experimental resolution curves of D1A and the high resolution powder diffractometer 3T2, at LLB, measured with TbIG, D_Q, accompanied with the average separation required for a "good

measurement" of adjacent reflections ($\Delta(Q)/p$, with p=0.5) for orthorhombic crystal structures (j=8) of primitive cell having volumes of 350, 500, 1000 and 1500 Å^3.

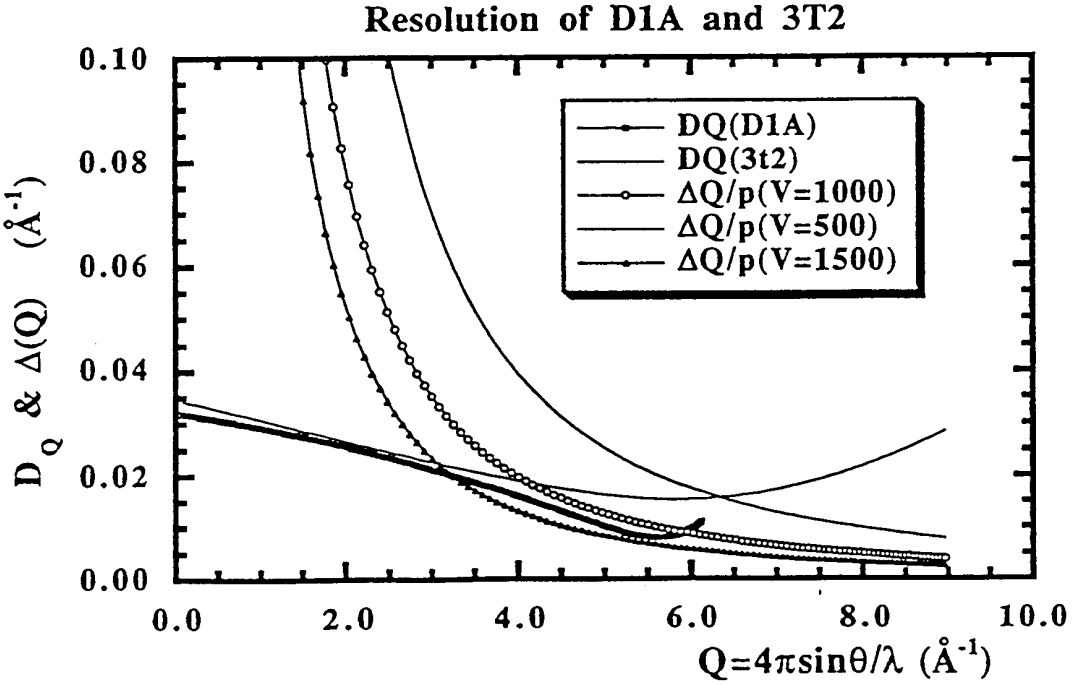

Figure 3: Comparison D1A(at l=1.98Å)-3T2

From the figure, it is worth mentioning that D1A at LLB is best suited for larger crystal structures than 3T2, due to a better resolution in its whole Q-range. On the contrary, for cells smaller that 300-400 Å^3, 3T2 can take advantage in refining the temperature factors, and providing more precise structural parameters, due to the larger Q-range available as a result of the smaller wavelength.

If there is no model for the structural problem the Rietveld method is not applicable. It is possible to obtain integrated intensities (for a single "phase") by refinement of the whole profile using $I_{\mathbf{H}}$ in expression [14] as least squares (LS) parameters, in order to try the *ab initio* resolution of the crystal structure. However, there is an intrinsic indetermination causing an infinite number of solutions (the matrix of the normal LS-equations is usually singular). When the reflections $\mathbf{H}_1$ and $\mathbf{H}_2$ are accidentally at the same position $T_{\mathbf{H}1}=T_{\mathbf{H}2}$ the global intensity $I(\mathbf{H}_1, \mathbf{H}_2)$ can be decomposed, $I_{\mathbf{H}1}+ I_{\mathbf{H}2}$, in an infinite number of ways. Usually the equipartition, $I_{\mathbf{H}1}= I_{\mathbf{H}2}$, is chosen. This uncertainty is the fundamental point limiting the capability of getting a structural solution from powder data. Another procedure to obtain integrated intensities is to iterate the calculated profile up to "match" the observed pattern.

The expression provided by Rietveld [32] (reference 7) to estimate the "observed" integrated intensity, I_j('obs'), in order to mimic the classical crystallographic R-factor (usually called R-Bragg):

$$I_j(\text{'obs'}) = \sum_i I_j(\text{calc})\, \Omega_{i,j}\ (y_{iobs} - B_i)/ (y_{ical} - B_i) \qquad [32]$$

can be written in iterative form for cycle "k" as:

$$I_j^k = \sum_i \Omega_{i,j} \{ (y_{iobs} - B_i)/ (y_{ical} - B_i) \}\ I_j^{k-1} \qquad [33]$$

Whatever Rietveld program can be easily modified to include the possibility of "fitting" the whole profile without structural model using the expression [33] for iterative calculation of the integrated intensities. Of course, the rest of profile parameters can be refined simultaneously with the usual LS procedure. The method of "profile matching" is extremely efficient and fast and provides a list of the integrated intensity of all the independent reflections within the measured angular range. Contrary to single crystal data, many reflections have wrong intensity as they overlap. To solve a crystal structure from such a reflection list one has to try different ways to distribute a "single observation" (intensity sum of a peak cluster) between several reflections, and then apply the usual single crystal methods (direct methods or Patterson synthesis, for instance). Due to the much better resolution, X-ray synchrotron radiation is more suitable for getting a good set of integrated intensities for crystal structure determination from powder data. Neutron powder diffraction takes the advantage in the refinement of the structure.
Several procedures have been proposed in order to distribute the intensity of a cluster between its components. The most simple one is based in the technique of "squaring" an initial Patterson map obtained from the equipartitioned data set: from the squared map new Fourier coefficients are obtained allowing a new distribuion for the overlapping reflections. This cycle is repeated until the statistical intensity distribution of the overlapping reflections is similar to that of the non-overlapping ones.

The reader interested in this subject can consult the articles given in reference 8 and the references therein.

4. Refinement of Crystal Structures by Neutron Powder Diffraction.

In the study of crystal structures, the best results can be obtained using single crystals. However, single crystals of suitable size are not always available; moreover, in most cases (defective materials) the actual nature of the compound makes the absence of such single crystals nearly intrinsic. The RM described in section 2 is commonly used for the analysis of powder diffraction patterns in order to refine crystal structures. The success of the RM in neutron diffraction was based in the easy modelling of the peak shape (gaussian) and the parametrization of the FWHM (see equation [23]). For many defective materials this approach is valid and the RM can be used to refine crystal structures getting, simultaneously, information about the nature and concentration of defects.

An example of that is shown in the next paragraph. Later we shall treat the case where anisotropic broadening of Bragg reflections modifies substantially the smooth behaviour given by [23].

4.1. POWDER DIFFRACTION OF DEFECTIVE MATERIALS WITH WELL RESOLVED BRAGG REFLECTIONS.

In the recent literature there is a great number of articles devoted to the structural study of defective materials by means of NPD. One of the most recent applications of the RM is the study of High-T_c superconductors, where the oxygen defects (vacancies or interstitials) determine to a large extent the actual T_c. The advantage of neutrons with respect to X-rays comes in this case from the higher relative scattering power of oxygen. The determination of the oxygen content, and the possible ordering of the vacancies, is one of the challenges for the researcher trying to understand the nature of superconductivity in these novel materials. The reader can find, for example in the journal Physica C, a huge number of articles on this subject.

Here, we want to show the particular example, which is also relevant to the next section, of the defect structure of $La_2NiO_{4+\delta}$. This is a semiconductor material related to the High-T_c superconductors $La_{2-x}Sr_xCuO_4$, but the oxygen excess is greater. The work of Jorgensen *et al.*[9] demonstrated the usefulness of NPD and the RM in the structural analysis of defects. The authors show that oxygen enters as interstitial in the position (1/4 1/4 z≈0.25) in the LaO layers, producing a displacement of the nearest oxygen atoms (see figure 4).

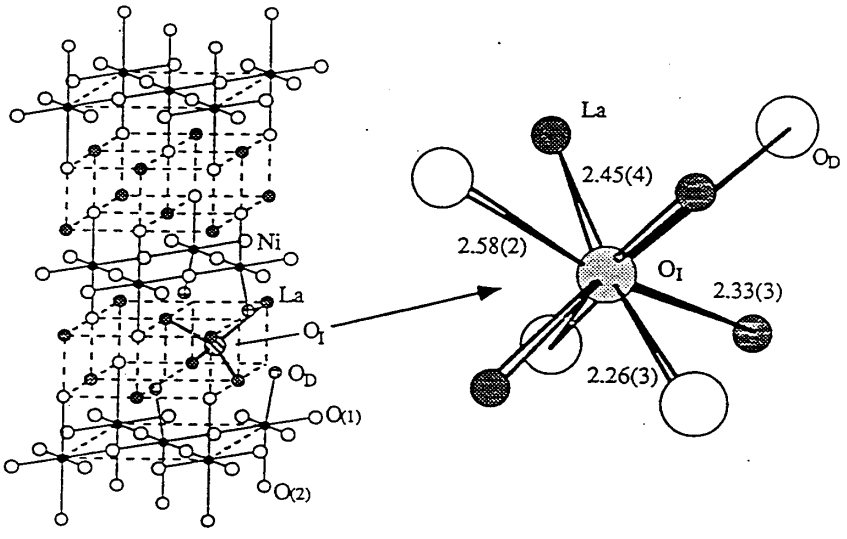

Figure 4: Structure of the interstitial oxygen in La_2NiO_{4+d} (from references 9 and 13).

4.2. THE USE OF THE EXTENDED RIETVELD METHOD TO DETERMINE THE MICROSTRUCTURE OF A MATERIAL. EXAMPLES.

In the previous paragraph we have treated the situations where the conventional RM can be applied, that is, where the profile function $\Omega(T)$ is only slightly affected by defects.

One of the most useful approximations is to consider that both, instrumental and intrinsic profiles can be well described by a Voigt function; i.e. a convolution of a gaussian and a lorentzian. The pseudo-Voigt function as described in 10, is a good numerical approximation. This is equivalent to assuming fixed size and strain distributions. The most direct quantity that can be obtained easily is the volume averaged domain size, and the root mean square microstrain, in the direction perpendicular to the (*hkl*) planes. These magnitudes are related to the integral breadth, $\beta_{\mathbf{H}}$, of the reflections through the relations:

$$\langle D \rangle = \lambda / \beta_{(size)} \cos\theta \qquad [34]$$

$$\varepsilon = k\, \beta_{(strain)} \tan\theta \qquad [35]$$

The constant k depends on the particular strain distribution assumed. Parameters describing isotropic strains and size effects have been introduced in the RM[11], through the scattering angle dependence of equations [34-35]. However, strains and size can give anisotropic broadening of Bragg reflections, and some Rietveld refinement programs can handle these effects[12].

The general treatment of anisotropic broadening in the RM, as is implemented in FullProf[12] is detailed in the Appendix. We shall give two examples in which this anisotropic broadening is due to strains, but the physical origin is different. The first one concerns the stoichiometric La_2NiO_4[13]. The compound is isomorphous to the parent La_2CuO_4 of a family of High-Tc superconductors; it crystallizes at room temperature in the group Bmab. The structure is a distortion of the tetragonal K_2NiF_4(I4/mmm) structural type. The crystals are micro-twinned in this Bmab phase with twin boundaries parallel to <110> directions. On cooling there is a first order structural phase transition, changing the direction of the octahedral tilt axis. The new average structure is tetragonal ($P4_2/ncm$). However, as explained in reference 13, strong microstrains appear at the transition as a consequence of the micro-twinned parent structure. In small regions, the local cell is orthorhombic with : $a_l = a_T(1-\varepsilon_l)$, $b_l = a_T(1+\varepsilon_l)$ and $c_l = c_T$, where ε_l is the local microstrain. This gives rise to a dependence of the broadening of Bragg reflections described by :

$$\mathrm{FWHM}(2\theta)_S = \{ [4\sqrt{(2\ln 2)}\, |h^2-k^2|\varepsilon] / [(h^2+k^2)+ (a_T^2/ c_T^2)l^2] \} \tan\theta \qquad [36]$$

The refinable microstrain parameter $\varepsilon = \langle \varepsilon^2_l \rangle^{1/2}$ depends on the interaction between the pre-existent twin boundaries. It has been proved that the larger the concentration of twin boundaries, the larger the value of the ε parameter. In figure 5 the dramatic effect, on the observed versus calculated profile, of the introduction of only one additional parameter can be observed.

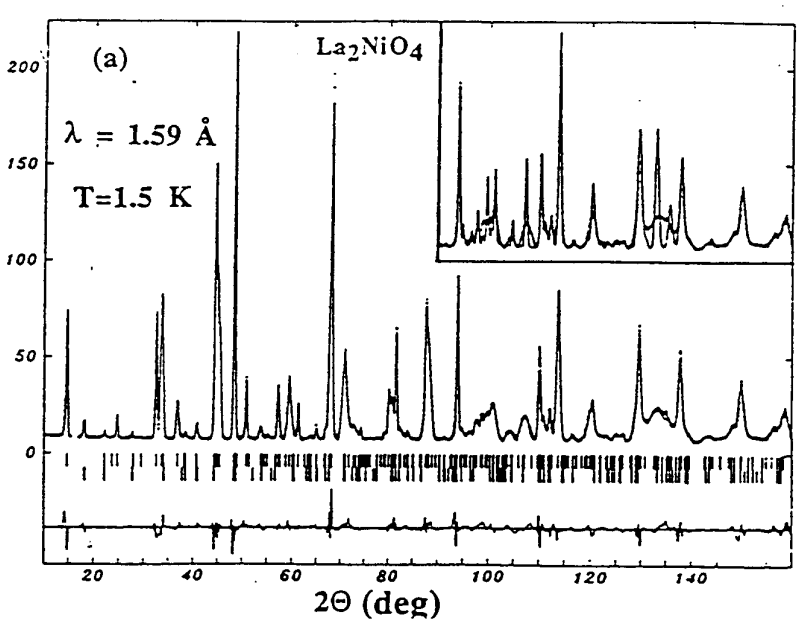

Figure 5: The neutron powder diffraction pattern of the low temperature phase of La_2NiO_4. In the inset is shown, as a comparison with the observed profile, a portion of the calculated pattern without the strain model discussed in the text.

The second example belongs also to the same family of materials. Substituting Sr for La in La_2NiO_4, it is possible to obtain a solid solution. If the samples are treated in a reducing atmosphere, oxygen vacancies are produced. The compound $La_{1.5}Sr_{0.5}NiO_{3.6}$ (Immm) derives from the parent K_2NiF_4-type structure by partial ordering of vacancies in the NiO_2 planes[14]. The larger number of vacancies is located in the site of the oxygen O(1/200), in such a way that the fully reduced compound should have a structure isomorphous to Sr_2CuO_3.

The incomplete reduction promotes fluctuations in the cell parameter *a*; the reflections of type (*0kl*) are normal, while those with $h \neq 0$ are broadened. The expression for the broadening is:

$$FWHM(2\theta)_S = \{ [4\sqrt{(2\ln 2)}\, h^2\, \varepsilon] / [a^2(h^2/a^2 + k^2/b^2 + l^2/c^2] \} \tan\theta \qquad [37]$$

In this case also, the improvement in the fit is conclusive, as can be seen in figure 6. The last two examples show that it is necessary to have a model for the anisotropic peak broadening in order to solve the average structure.

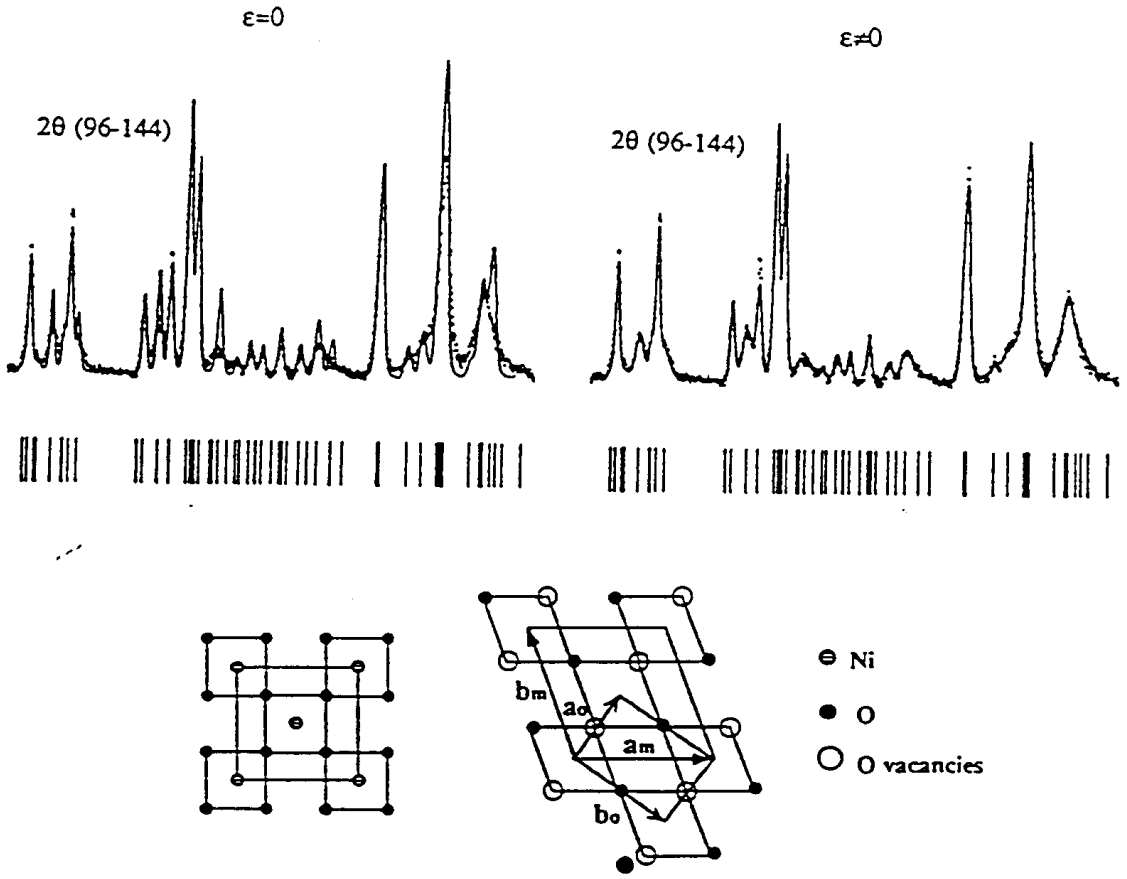

Figure 6: Portions of the neutron powder diffraction pattern of the compound $La_{1.5}Sr_{0.5}NiO_{3.6}$ showing the effect of the microstrain due to the partial ordering of the oxygen vacancies (reference 14). The scheme on the left shows the ideal NiO_2 basal plane. On the right, an exaggerated view of the deformation of the NiO_{2-x} plane is shown.

Appendix

EXPRESSION OF BROADENING DUE TO CELL PARAMETER FLUCTUATIONS.

It can be demonstrated that, except for a scaling term, the intrinsic profile function reproduces the distribution function of the microdistortions (see Guinier pp 243-244). We shall make the hypothesis that the particular defects existing in the sample produce correlated fluctuations of cell parameters of gaussian character. Then, if x represent a "cell parameter" (direct or reciprocal) of

mean α and variance $\sigma^2(\alpha)$, the probability of finding the value "x" is given by the normal distribution:

$$P(x)= 1/\sqrt{(2\pi)}/\sigma(\alpha)\ \exp\{-1/2\ [(x-\alpha)/\sigma(\alpha)]^2\} \qquad [A1]$$

The fullwith at half maximum (H=FWHM) is related to the variance by the expresion $H=2\sqrt{(2\ln 2)}\sigma(\alpha)$. Let us calculate the variance of the square[15] of the scattering vector for the reflection (hkl) as a function of the variances and co-variances of the cell parameters . The relevant function is:

$$s^2= 1/d^2 = M(x_i; hkl) \qquad [A2]$$

where $\{x_i\}$ (i=1,2,...6) are direct or reciprocal cell parameters, or, in general any set of six parameters defining the metrics of the unit cell. The parameters $\{x_i\}$ are considered as normally distributed random variables of mean values $\{\alpha_i\}$, with a covariance matrix of components S_{ij} = $\mathrm{cov}(x_i, x_j)$ [$\mathrm{cov}(x_i, x_i) = \sigma^2(\alpha_i)$]. The correlation matrix is defined from S_{ij} by $C_{ij} = \mathrm{corr}(x_i, x_j) = \mathrm{cov}(x_i, x_j)/[\sigma(\alpha_i)\sigma(\alpha_j)]$. The mean value of M and its variance are given by:

$$M_{hkl} = M(\alpha_i; hkl)$$
$$\sigma^2(M_{hkl}) = \sum\sum S_{ij}\ (\partial M/\partial\alpha_i)(\partial M/\partial\alpha_j) \qquad [A3]$$

Where we have put : $\partial M/\partial\alpha_i = (\partial M/\partial x_i)_{Xi=\alpha i}$. If another set of parameters $p_k= p_k(x_i)$ is used, the relation betwen their respective covariance matrices is the following:

$$\sigma^2(M_{hkl}) = \sum\sum S_{ij}\ \partial M/\partial\alpha_i\ \partial M/\partial\alpha_j = \sum\sum S_{ij} \sum \partial M/\partial\pi_k\ \partial p_k/\partial\alpha_i \sum \partial M/\partial\pi_n\ \partial p_n/\partial\alpha_j$$
$$=\sum\sum(\sum\sum\partial p_k/\partial\alpha_i\ S_{ij}\ \partial p_n/\partial\alpha_j)\ \partial M/\partial\pi_k\ \partial M/\partial\pi_n$$
$$=\sum\sum S'_{kn}\ \partial M/\partial\pi_k\ \partial M/\partial\pi_n \qquad [A4]$$

The peak shape produced by the normal distribution [A1] is gaussian, then the FWHM can be easily calculated from the variance. The Bragg law allows to relate the variance of M with the FWHM of the reflection due to strains in the angular space:

$$H^2_s = (8\ln 2)\sigma^2(2\theta)_s = (8\ln 2)\sigma^2(M_{hkl}) / M_{hkl} \tan^2\theta \qquad [A5]$$

This strain contribution must be added to the instrumental parameter U in the Caglioti expression in order to obtain the experimental FWHM:

$$H = U + (8\ln 2)\sigma^2(M_{hkl}) / M_{hkl} \tan^2\theta + V \tan\theta + W \qquad [A6]$$

The establishement of a "microstrain model" explaining the experimental data is equivalent to find the values of the covariance matrix and relate these values to the particular defects existing in the sample. This corresponds to give a physical interpretation of the results, task that could be not obvious at all. We shall calculate explicit forms of $\sigma^2(M_{hkl})/M_{hkl}$ for particular cases without description of the physical origin of the fluctuations.

Tetragonal lattice with correlated orthorhombic distortions.

This case correspond to one of the examples dicussed in the text. In this case we use the direct cell parameters:
$\langle a\rangle = \langle b\rangle = a_T$, $\langle c\rangle = c_T$, $\sigma^2(a) = \sigma^2(b) = \sigma^2$, $\sigma^2(c) = 0$, $\mathrm{cov}(a,b) = -\sigma^2$ ($\mathrm{corr}(a,b) = -1$)

Using the formula [A3] and the microstrain parameter $\varepsilon = \sigma/a_T$ one obtains:

$$\sigma^2(M_{hkl}) = 4\,(h^2 - k^2)^2\sigma^2 / a_T^6 = 4\,(h^2 - k^2)^2\varepsilon^2 / a_T^4$$

The FWHM of the reflections is given by the expression [36] in the text.

General distortions in an hexagonal lattice.

We shall use, instead of the direct cell parameters, the coefficients of the quadratic form

$$M_{hkl} = A(h^2 + k^2 + hk) + C\,l^2$$

Using the same notations as above, the variance of M is:

$$\sigma^2(M_{hkl}) = (h^2 + k^2 + hk,\ l^2) \begin{pmatrix} S_A & C_{AC} & h^2 + k^2 + hk \\ C_{AC} & S_C & l^2 \end{pmatrix}$$

$$\sigma^2(M_{hkl}) = S^2_{AA}\,(h^2 + k^2 + hk)^2 + S^2_{CC}\,l^4 + 2C_{AB}S_{AA}S_{CC}(h^2 + k^2 + hk)l^2$$

When using the fluctuations of the coefficients of the quadratic form M_{hkl} one has to interpret what happens in the real space, in terms of fluctuations of direct cell parameters. It is easy to obtain,

by applying the formula A2, the variance co-variance matrix corresponding to the direct cell parameters as a function the three parameters S_{AA}, S_{CC} and C_{AB}, which are the actual fitted parameters. The fluctuations and correlation of the direct cell parameters are:

$$\sigma(a) = 3a^3/8\ S_A \qquad\qquad \sigma(c) = c^3/2\ S_C \quad C_{ac} = C_{AC}$$

The parameters that are directly fitted by the program are S_{AA} , S_{CC} and C_{AB}.
The reader can verify that our formulation, except for an overall isotropic term, is equivalent to that of reference 16. The advantage of our formalism stems from a simpler interpretation of the refined strain parameters. The overall isotropic strain is absorbed in the value of U in A6, it expression (when U is given in degrees^2) is:

$$[\sigma(M)/M]_{iso} = \pi/180\ \sqrt{(U_{ref} - U_{ins})}/(8\ln 2) = 174.53\ \sqrt{(U_{ref} - U_{ins})}$$

General distortions in an orthorhombic lattice.

We shall use, instead of the direct cell parameters, the coefficients of the quadratic form

$$M_{hkl} = A\ h^2 + B\ k^2 + C\ l^2$$

The following notation is used $\sigma^2(A) = S_A$, $\partial M/\partial A = h^2$, $Cov(A,B) = C_{AB}$, etc. The variance of M is:

$$\sigma^2(M_{hkl}) = (\ h^2,\ k^2\ ,\ l^2\ ) \begin{matrix} S_A & C_{AB} & C_{AC} \\ C_{AB} & S_B & C_{BC} \\ C_{AC} & C_{BC} & S_C \end{matrix} \begin{matrix} h^2 \\ k^2 \\ l^2 \end{matrix}$$

$$\sigma^2(M_{hkl}) = S_A\ h^4 + S_B\ k^4 + S_C\ l^4 + 2[C_{AB}\ h^2\ k^2 + C_{AC}\ h^2\ l^2 + C_{BC}\ k^2\ l^2\ ]$$

In general, the parameters S_i and C_{ij} can be refined directly in the modified Rietveld Method. For the othorhombic lattice described, as an example, in the text it is easy to see that the model corresponds to all S_i and C_{ij} equal to zero except for S_A .

References

[1] **A. Guinier**, *X-ray Diffraction in Crystals, Imperfect Crystals, and Amorphous Bodies*, W.H. Freeman and Company, San Francisco, USA (1963).
B.E. Warren, *X-ray Diffraction*, Addison Wesley, Massachusetts, USA (1969).
J.M. Cowley, *Diffraction Physics*, North Holland, Amsterdam (1975).
S. W. Lovesey, *Theory of Neutron Scattering from Condensed Matter*, Vol.1,2. Clarendon Press, Oxford, 1986

[2] **B.T.M. Willis & A.W. Pryor**, *Thermal Vibration in Crystallography* , Cambridge University Press, 1975.

[3] **B.E.F. Fender**, *Diffuse Scattering and the Study of Defect Solids*, in Chemical Applications of Thermal Neutron Scattering, pp 250-270, ed. B.T.M Willis, Oxford University Press (1973)

[4] **H.M. Rietveld**, *A Profile Refinement Method for Nuclear and Magnetic Structures*, J. Appl. Cryst. **2**, 65 (1969)

[5] **A.K. Cheetham and J.C. Taylor**, *Profile Analysis of Powder Neutron Diffraction Data: Its Scope, Limitations, and Applications in Solid State Chemistry*, J. Solid State Chem., **21**, 253 (1977).
A. Albinati and B.T.M. Willis, *The Rietveld Method in Neutron and X-ray Powder Diffraction*, J. Appl. Cryst. **15**, 361 (1982)
A. W. Hewat, *High-Resolution Neutron and Synchrotron Powder Diffraction*,Chemica Scripta **26A**, 119 (1985)
The Rietveld Method, edited by **R.A. Young.** International Union of Crystallography, Oxford Science Publications, (1996)

[6] **U.H. Zucker and H. Schulz**, *Statistical Approaches for the Treatment of Anharmonic Motion in Crystals* I and II, Acta Cryst. A38, 563&568 (1982).

[7] **A.W. Hewat,** *Design of a conventional high-resolution neutron powder diffractometer*, Nucl. Inst. and Meth., **127**, 361 (1975)
W.I.F. David, D.E. Akporiaye, R.M. Ibberson and C.C. Wilson, *The High Resolution Powder Diffractometer at ISIS - An Introductory Users Guide*, Internal Report, RAL-88-103, December 1988.

[8] **G.Cascarano, L. Favia and C. Giacovazzo**, *SIRPOW.91- a Direct-Methods Package Optimized for Powder Data*, J. Appl. Cryst. **25**, 310 (1992).
M.A. Estermann, L.B. MacCusker and C. Baerlocher, *Ab Initio Structure Determination from Severely Overlapping Powder Diffraction Data*, J. Appl. Cryst. **25**, 539 (1992).

[9] **J.D. Jorgensen, B. Dabrowski, Shiyou Pei, D.R. Richards and D.G. Hinks**,

The Structure of the Interstitial Oxygen Defect in $La_2NiO_{4+\delta}$, Phys. Rev. **B 40**, 2187 (1989).

[10] **P. Thompson, D.E. Cox & J.B. Hastings**, *Rietveld Refinement of Debye-Scherrer Synchrotron X-ray Data from* Al_2O_3, J. Appl. Cryst. **20**, 79 (1987)

[11] **Th.H. de Keijser, E.J. Mittemeijer & H.C.F. Rozendaal**, *The Determination of Crystallite-Size and Lattice-Strain Parameters in Conjunction with the Profile-Refinement Method for the Determination of Crystal Structures*, J. Appl. Cryst. **16**, 309 (1983)

[12] **A.C. Larson and R.B. Von Dreele**, GSAS *Generalized Structure Analysis System*, Laur 86-748. Los Alamos National Laboratory, Los Alamos, NM 87545.
J. Rodríguez-Carvajal, FULLPROF: *A Program for Rietveld Refinement and Pattern Matching Analysis*". Abstracts of the Satellite Meeting on Powder Diffraction of the XVth Congress of the International Union of Crystallography. p.127. Toulouse, 1990.

[13] **J.Rodríguez-Carvajal, M.T.Fernández-Díaz and J.L.Martínez**, *Neutron diffraction study on structural and magnetic properties of* La_2NiO_4, J. Phys.: Condensed Matter **3**, 3215 (1991).

[14] **M. Medarde, J. Rodríguez-Carvajal, X. Obradors, J. González-Calbet, M. Vallet & M.J. Sayagués**, *Oxygen Vacancy Ordering in* $La_{2-x}Sr_xNiO_{4-\delta}$, Physica B **180**&**181**, 399 (1992).

[15] It is much more convenient to use s^2 instead of s for calculating the spread of the Bragg reflection in reciprocal space as a function of the variances of the primary cell parameters.

[16] **P. Thompson, J.J. Reilly & J.M. Hastings**, *The accommodation of strain and particle broadening in Rietveld refinement: its application to de-deuterized lanthanum nickel (*$LaNi_5$*) alloy* J. Less Common Metals **129**, 105 (1987)